International Journal of Molecular Sciences

MDPI

Article

Gamma Irradiation Processing on 3D PCL Devices - A Preliminary Biocompatibility Assessment

Fernando Guedes [1,2,3], Mariana V. Branquinho [1,2,3], Sara Biscaia [4], Rui D. Alvites [1,2,3], Ana C. Sousa [1,2,3], Bruna Lopes [1,2,3], Patrícia Sousa [1,2,3], Alexandra Rêma [1], Irina Amorim [6,7], Fátima Faria [5], Tatiana M. Patrício [4], Nuno Alves [4], António Bugalho [7,8] and Ana C. Maurício [1,2,3]

1 Veterinary Clinics Department, Abel Salazar Biomedical Sciences Institute (ICBAS), University of Porto (UP), Rua de Jorge Viterbo Ferreira, nº 228, 4050-313, Porto, Portugal; fernando.t.guedes@gmail.com (F.G.) m.esteves.vieira@gmail.com (M.V.B.); ruialvites@hotmail.com (R.D.A.). anacatarinasoaressousa@hotmail.com (A.C.S.); brunisabel95@gmail.com (B.L.); pfrfs_10@hotmail.com (P.S.); alexandra.rema@gmail.com (A.R.); acmauricio@icbas.up.pt (A.C.M.).

2 Animal Science Studies Centre (CECA), Agroenvironment, Technologies and Sciences Institute (ICETA), University of Porto, Rua D. Manuel II, Apartado 55142, 4051-401, Porto, Portugal.

3 Associate Laboratory for Animal and Veterinary Science (AL4AnimalS), Lisbon, Portugal.

4 Centre for Rapid and Sustainable Product Development (CDRSP), Polytechnic Institute of Leiria, 2411-901 Leiria, Portugal; sara.biscaia@ipleiria.pt (S.B.); tatiana.patricio@ipleiria.pt (T.P.); nuno.alves@ipleiria.pt (N.A.).

5 Department of Pathology and Molecular Immunology, Abel Salazar Institute of Biomedical Sciences (ICBAS), University of Porto (UP), Rua Jorge Viterbo Ferreira, n ° 228, 4050-313, Porto, Portugal; irinamorim@hotmail.com (I.A.) fatimafaria10@yahoo.com.br (F.F.).

6 Institute of Research and Innovation in Health (i3S), University of Porto (UP), Rua Alfredo Allen, 4200-135, Porto, Portugal.

7 CUF Tejo Hospital and CUF Descobertas Hospital, Lisbon, Portugal; antonio.bugalho@gmail.com (A.B.).

8 Center of Studies for Cronic Diseases (CEDOC), NOVA Medical School, Lisbon, Portugal.

* Correspondence: Ana Colette Maurício
Departamento de Clínicas Veterinárias
Instituto de Ciências Biomédicas Abel Salazar (ICBAS), Universidade do Porto (UP).
Rua de Jorge Viterbo Ferreira, nº 228, 4050-313 Porto, Portugal.
Mobile: +351.91.9071286 ; Phone: +351.22.0428000
Email: ana.colette@hotmail.com, acmauricio@icbas.up.pt

Abstract: Additive manufacturing or 3D printing applying polycaprolactone-(PCL)-based medical devices represents an important branch of tissue engineering, where the sterilization method is a key process for further safe application *in vitro* and *in vivo*. In this study, the authors intend to access the most suitable gamma radiation conditions to sterilize PCL-based scaffolds in a preliminary biocompatibility assessment, envisioning future studies for airway obstruction conditions. Three radiation levels were considered, 25 kGy, 35 kGy and 45 kGy and evaluated as to their cyto- and biocompatibility. All three groups presented biocompatible properties, indicating an adequate sterility condition. As for the cytocompatibility analysis, devices sterilized by 35 kGy and 45 kGy showed better results, with the 45 kGy showing overall improved outcomes. This study allowed to select the most suitable sterilization condition for PCL-based scaffolds, aiming at immediate future assays, by applying 3D-customized printing techniques to specific airway obstruction lesions of the trachea.

Keywords: gamma irradiation; 3D polycaprolactone; mesenchymal stem cells; cytocompatibility; biocompatibility.

1. Introduction

 doi:10.20944/preprints202210.0202.v1

Several fabrication techniques have been used to create clinically applicable scaffolds with uniform pore size and control over geometry. Additive manufacturing (AM), also known as 3D printing, enables customize fabrication of 3D constructs based on computer-aided design software or images obtained from computer tomography and magnetic resonance. There are several AM techniques, among which only some techniques are widely applied in the medical industry [1]. The most widely used are droplet-based printing [2], and extrusion-based printing [3]. Tissue engineering (TE) with 3D printing is focused on two different perspectives: functional biomaterials for tissue implantation and tissue models for disease [1]. This study will focus on biomaterials based on the first option.

Scaffolds have found their place as templates for cell interaction, providing physical support to the afresh developed tissue [3]. Furthermore, scaffolds can function as delivery vehicles to incorporate essential growth factors and biomolecules to control and enhance tissue growth [4]. The aim of 3D bioprinting is to mimic the natural cellular architecture by depositing materials and cells to restore the normal structure and functionality of complex tissues. TE scaffolds are fabricated in two major methods, printing with cells mixed in ink or gel or seeding cells onto scaffolds post printing [4].

The role of airway TE, a field of regenerative medicine, is to develop biological substitutes that can restore, maintain, or improve tissue functions. As a "simple" cylinder and with a relatively main function, which is to conduct the air, trachea was initially considered as a good starter organ for TE and historically many attempts were made with autografts, allografts, and prosthetic materials [5, 6]. The ideal tissue engineered scaffold for airway would be capable of promoting exogenous cell engraftment and endogenous cell ingrowth, proliferation, and appropriate differentiation, while maintaining a patent airway.

In the context of airway TE, central airway obstruction (CAO) represents a pathological condition that leads to airflow limitation of the trachea, main stem *bronchi*, *bronchi intermedius* or *lobar bronchus*. That represents an important clinical impairment and can be caused either from benign or malignant diseases [7, 8]. The incidence is still not well known, but it tends to be underdiagnosed [9]. While the surgical procedure is considered the gold standard, several clinical conditions concerning the clinical condition of the patient, the degree and the type of CAO could compromise the feasibility of the standard therapy [10]. In those cases, interventional bronchology with its accessory techniques such as laser, cryotherapy dilatation or airway stenting could represent a good option [11, 12]. Airway stenting could be used in both benign and malign disease, but placing the stent must be a very well balanced decision because if for one hand the re-occlusion is prevented, on the other hand it has also disadvantages such as stent migration, mucous plugging, recurrent infection or fistulation [10, 13]. There are two main types of airway stenting concerning the material: silicone stents and metallic stents. new custom-made and bioabsorbable airway stents made of different biomaterials are under investigation and have been placed in humans. Polydioxanone is the one that has been most often used and for the longest period [14]. Other biomaterials like polylactic acid, polyglycolic acid, polycaprolactone, polyurethane or polyamide are under investigation [15, 16]. Biodegradable polymers such polycaprolactone (PCL) are increasingly used for 3D printing of scaffolds. This material offers great advantages such as biocompatibility, biodegradability, and good mechanical properties [17]. However, to be approved for human implantation, they must be in sterile conditions. Numerous techniques have been researched, all of them subject of limitations [18]. The most frequently used are ethylene oxide, beta radiation, gamma radiation, peracetic acid and hydrogen-peroxide plasma. Steam and heat sterilization are not practicable in this polymer as it has a melting point of 59-64ºc. Ethylene oxide could be an option, but it is known to soften PCL and its residual vapors left in the device found to be mutagenic and carcinogenic [19]. Thus, ionizing is likely the method of choice and gamma radiation represents the most extensively studied sterilization method for PCL [20, 21]. Gamma radiation is highly penetrative and kills

 doi:10.20944/preprints202210.0202.v1

bacteria by breaking down bacterial DNA, thereby inhibiting bacterial division. On the other hand such photon-induced damage at the molecular level can also cause changes in the physical and chemical properties of the polymer. A minimum dose of 25kGy is routinely applied for sterilization of many medical devices and biological tissues. As recommended by the International Organization of Standardization (ISO), the sterilization dose must be set for each type of product depending on its characteristics and the load of microbes [20].

The most important properties of a bioabsorbable scaffold are the degradation rate, mechanical strength, and ability to support cell growth. Gamma rays at 30.8 kGy significantly decrease the rate of degradation of PCL, without affecting molecular weight nor cells attachment and growth. Considering mechanical properties, yield stress increased significatively but not the stress at break. In the case of the scaffold it represents an important support rule as in the airway, this is of the upmost relevance [22]. Augustine *et al* report a low radiation dose first would lead to improved PCL mechanical properties, however, higher doses would decrease them. Thus, results for the effect of gamma radiation on the mechanical properties are ambiguous and a general trend has not yet been established.

In this preliminary work the authors intended to study the cytocompatibility and biocompatibility of 3D printed polycaprolactone (PCL) based devices [23] after different gamma radiation conditions. The choice for the biomaterial relied on the premise that, in future assays, the device to be studied to promote regeneration of tracheal tissue must have a design that mimics the anatomical shape of trachea, must have mechanical strength and flexibility like native trachea and porosity that allows good vascularization and cell proliferation. In addition, it must be biocompatible, biodegradable and non-immunogenic [24]. Furthermore, PCL allows the production of 3D devices with interconnected porous network and high reproducibility [25]. Following the biomaterial production and characterization studies, *in vitro* and *in vivo* assays were conducted as to assess on the gamma radiation effect on the device's properties, the first applying mesenchymal stem cells (MSCs) from the dental pulp tissue of human origin and the latter considering subcutaneous implantation on a rat animal model.

2. Results

2.1. Devices Characterization

Fourier-transform infrared spectroscopy (FTIR) spectra of the scaffolds sterilized with different conditions are depicted in Figure 1. All samples present similar results in terms of chemical structure, with the characteristic bands of pure PCL. The bands at 2865 and 2941 cm−1 are related with the symmetric and asymmetric stretching of the CH2 group. A strong absorbance at 1720 cm^{-1} also corresponds to a structural group of PCL, more precisely C=O stretching vibration of the ester linkages. Figure 2 shows the results of the SEM examination of the PCL scaffolds gamma irradiated up to 45 kGy. All samples present micropores in the filament surface, indicating that the sterilization at 25, 35 and 45 kGy has no effect on the morphology of the filaments.

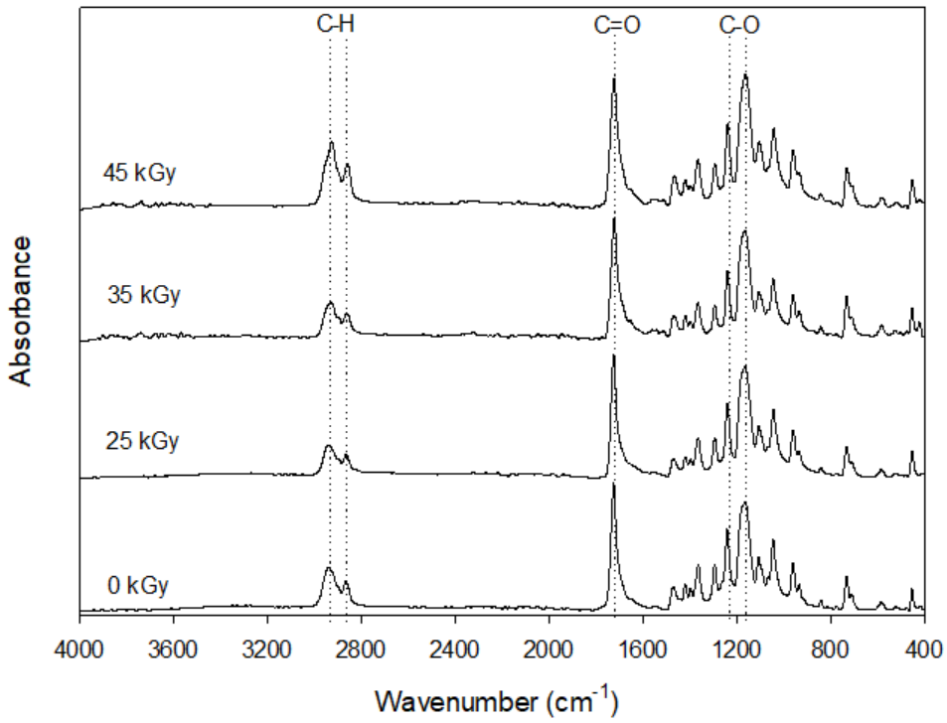

Figure 1. FTIR spectra of PCL scaffolds sterilized with different gamma radiation conditions.

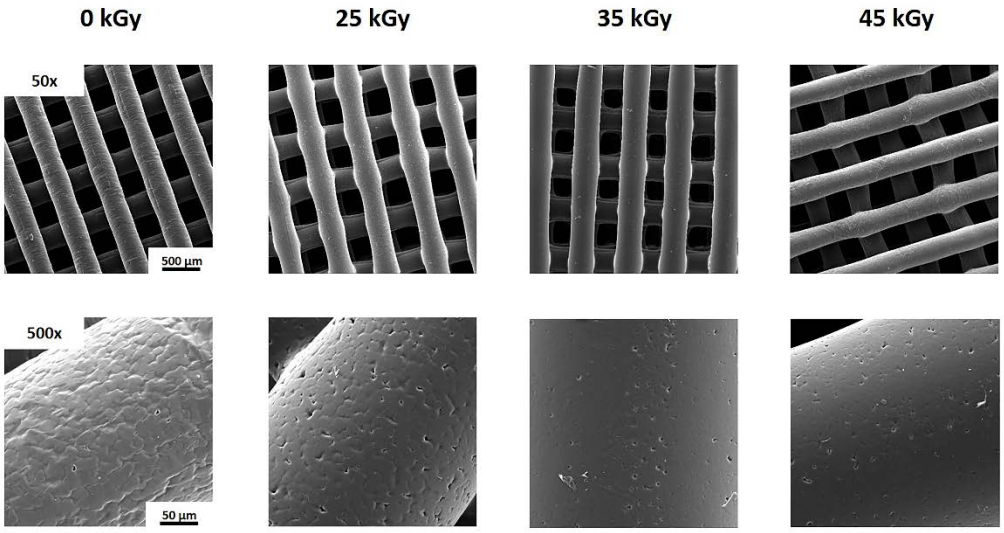

Figure 2. SEM images of gamma sterilized and unsterilized PCL scaffolds.

2.2. In vitro cytocompatibility assessment

A PrestoBlue™ cytocompatibilty assessment was conducted on the produced scaffolds, following sterilization. Scaffolds were divided into three groups, considering 3 different levels of sterilization: 25 kGy, 35 kGy and 45kGy. A control group of the cell population was considered, by seeding cells directly to the well with no scaffold, as to access cell normal behaviour and proliferation in culture. For each time-point, corrected absorbance values were obtained for each group and are presented in Figure 3 (upper panel) and Table 1.

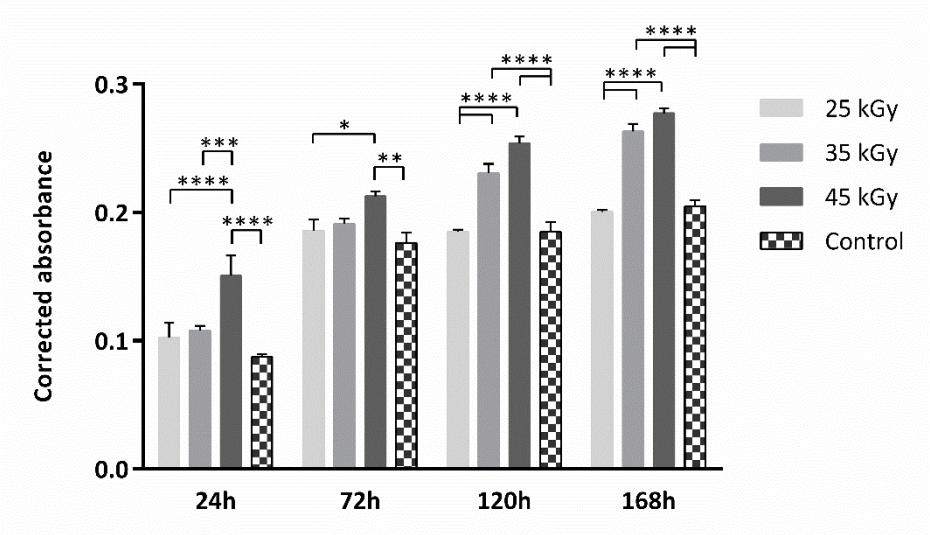

Figure 3. Presto Blue™ cytocompatibility assessment with hDPSCs. Results presented as mean ± SE. Results' significance is presented through the symbol (*), according to the p value, with one, two, three or four symbols, corresponding to $0.01 < p \leq 0.05$; $0.001 < p \leq 0.01$; $0.0001 < p \leq 0.001$; and $p \leq 0.0001$, respectively.

Table 1. Presto Blue™ cytocompatibility assessment with hDPSCs. Results presented as mean ± SE.

	25 kGy	35 kGy	45 kGy		Control
24h	0.102 ± 0.012	0.108 ± 0.003	0.151 ± 0.016		0.087 ± 0.002
72h	0.186 ± 0.009	0.191 ± 0.004	0.213 ± 0.004		0.176 ± 0.008
120h	0.185 ± 0.002	0.231 ± 0.007	0.254 ± 0.005		0.185 ± 0.007
168h	0.200 ± 0.002	0.263 ± 0.006	0.277 ± 0.004		0.205 ± 0.005

Human dental pulp stem/stromal cells (hDPSCs) were employed in this assay, following previous works [26-28]. These cells' population regenerative potential towards the osteogenic lineage has been established by Campos *et al* [29] and was selected for the purpose of this study, as the authors intend to further analyse the regenerative potential of PCL-based devices for tracheal airway-obstruction cases.

Following the Presto Blue™ cytocompatibility assessment, samples were processed for Scanning Electronic Microscopy (SEM). Seeded and unseeded devices were considered. Images are presented in Figure 4.

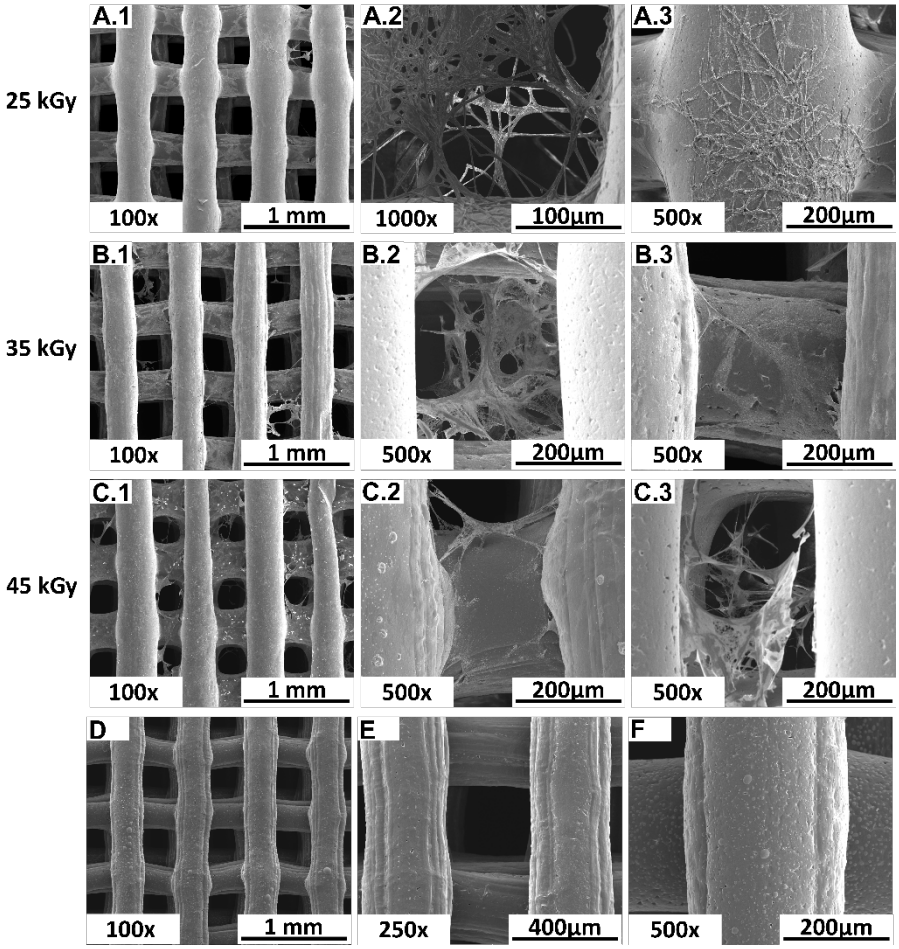

Figure 4. SEM images obtained from the 3D PCL devices seeded with hDPSCs. A, B and C representing seeded scaffolds sterilized by 25 kGy gamma radiation 35 kGy and 45 kGy, respectively. D, E and F represent the unseeded devices, sterilized by 25 kGy gamma radiation 35 kGy and 45 kGy, respectively. Left panel with 100x magnification and middle and right panel with 500x magnification.

SEM analysis allowed to visualize adhered cells to all the devices, presenting a fibroblast-like shape, normal morphology and adequate adhesion. Cells presented elongations of the cytoplasm, creating adhesion points between the device's fibers, thus creating a 3D cellular network. No differences could be qualitatively established between groups.

2.3. In vivo biocompatibility assessment

Following the *in vitro* assessment, devices were further assessed *in vivo* for their biocompatibility, according to ISO 10993-6:2016 guidelines for Biological evaluation of medical devices, Part 6: Tests for local effects after implantation. Scaffolds were implanted subcutaneously on the dorsum of Sasco Sprague-Dawley rats and analysed after 7 and 15 days post-implantation time. A semi-quantitative scoring analysis was performed, according to annex E of the referred guideline. Evaluation of the biological reaction to the devices included quantification of fibrosis, extent, inflammatory cells, necrosis, neovascularization, fat tissue infiltration, among others. Results are presented in Figure 6 and 7 and Table 2. Furthemore, samples were embedded in paraffin and analysed by SEM. The obtained images are presented in Figure 5.

 doi:10.20944/preprints202210.0202.v1

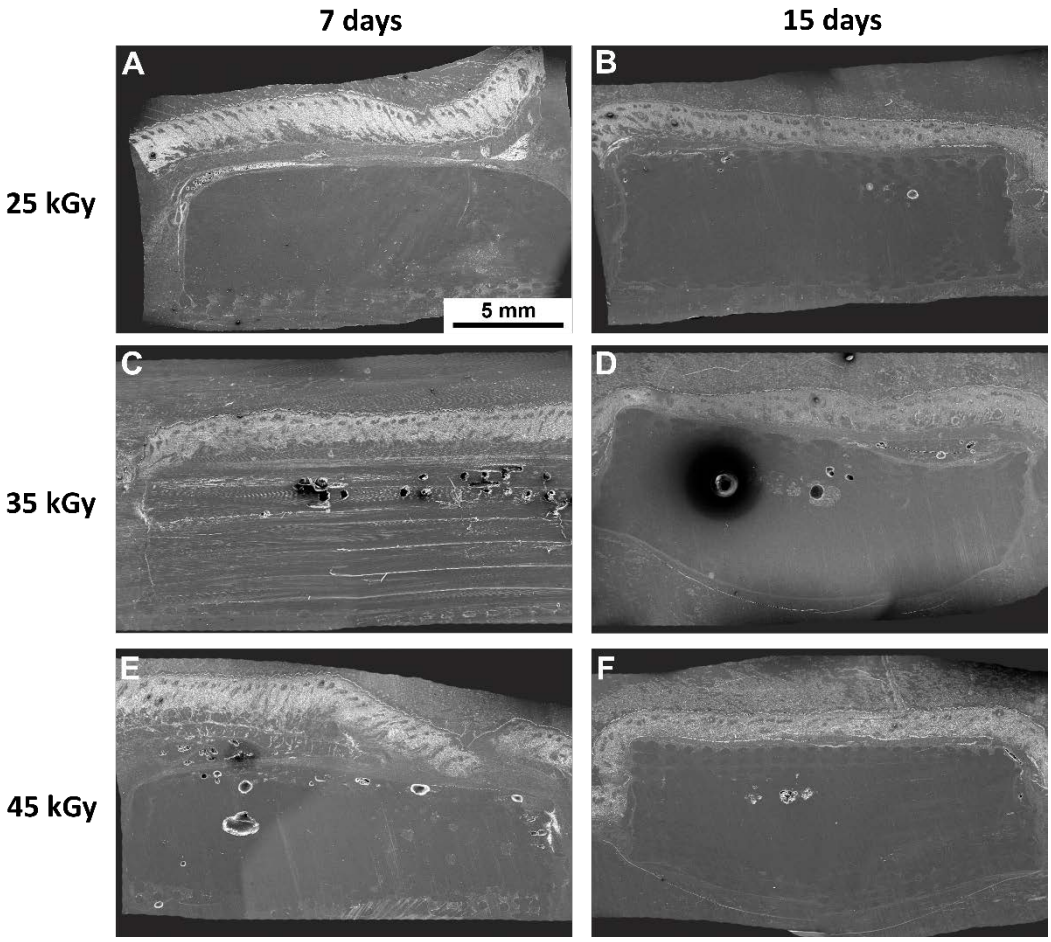

Figure 5. SEM images of the subcutaneously implanted 3D PCL devices in the rat animal model. Representing the left panel and the right panel, 7 days, and 15 days recovery time, respectively. A and B devices were sterilized by 25 kGy gamma radiation, C and D by 35 kGy and E and F by 45 kGy. Magnification of 20x and scale bar 5 mm.

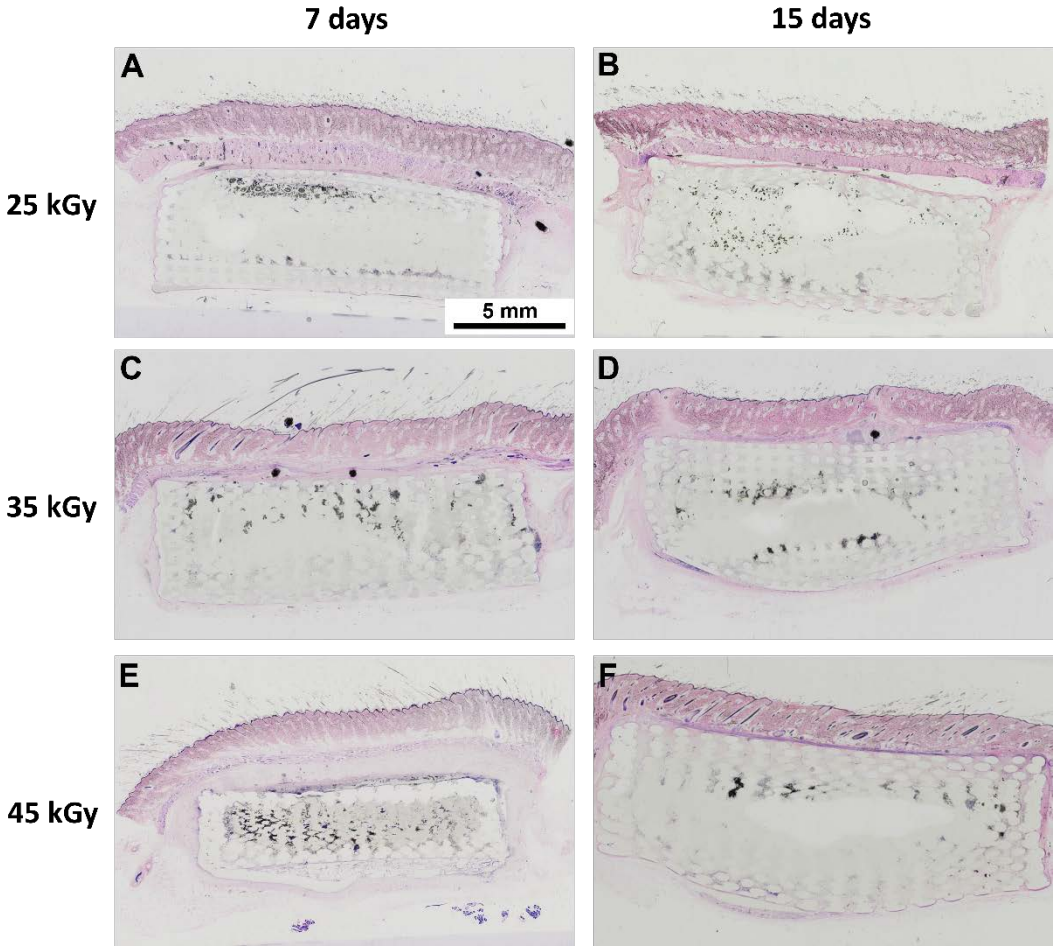

Figure 6. Histological images, stained with H&E, scanned using an Olympus Virtual Microscopy System VS110TM at 20x magnification, of the subcutaneously implanted 3D PCL scaffolds in the rat animal model. Representing the left panel and the right panel, 7 days, and 15 days recovery time, respectively. A and B scaffolds were sterilized by 25 kGy gamma radiation, C and D by 35 kGy and E and F by 45 kGy. Scale bar 5 mm.

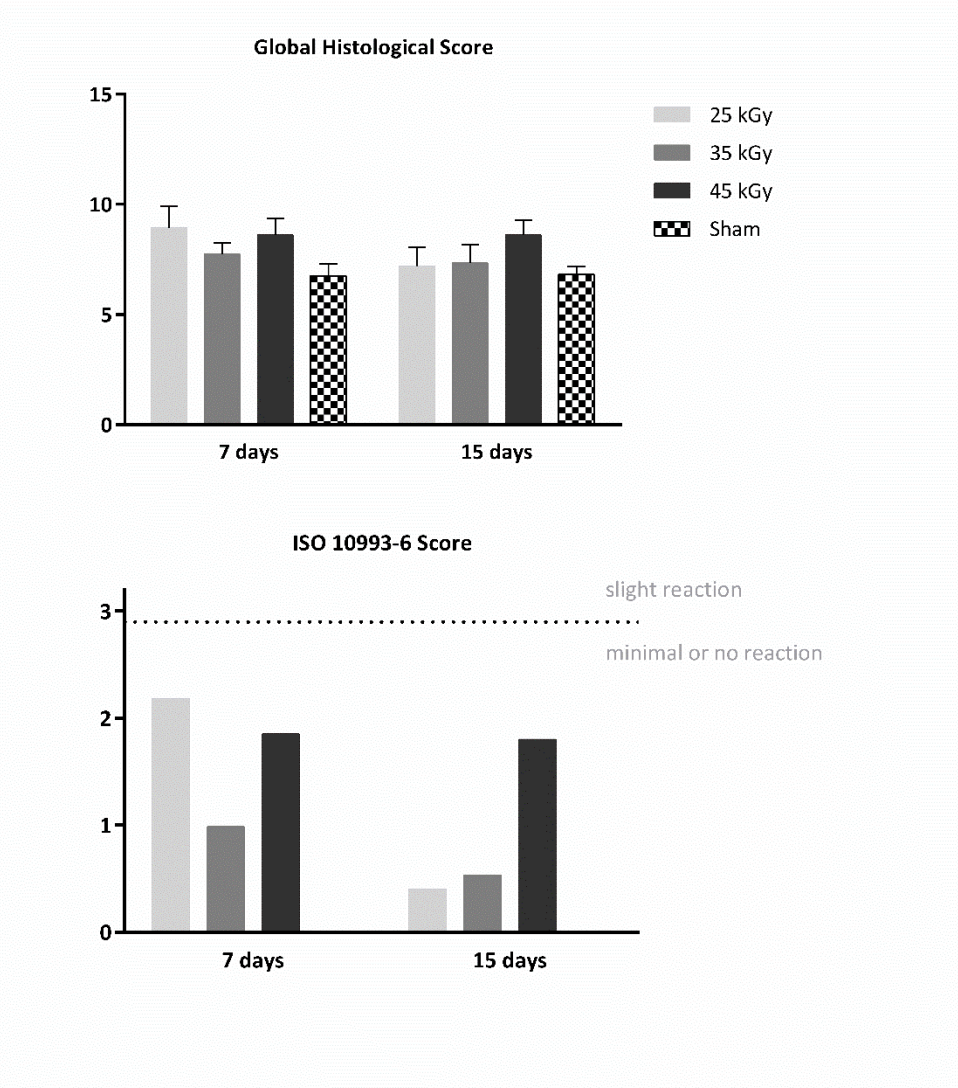

Figure 7. Global histological score (upper panel) and calculated score, according to guideline ISO 10993-6:2016 (lower panel), for subcutaneous implantation (biocompatibility assessment) of the PCL devices, after 7- and 15-days implantation time.

Table 2. Global histological scores presented as mean ± SE following ISO-10993-6 guidelines for the PCL devices groups and sham, at 7 and 15 days after implantation.

	Sham	25 kGy	35 kGy	45 kGy
7 days	6.750 ± 0.532	8.933 ± 0.959	7.733 ± 0.521	8.600 ± 0.748
ISO SCORE	-	**2.183**	**0.983**	**1.850**
15 days	6.800 ± 0.396	7.200 ± 0.846	7.333 ± 0.826	8.600 ± 0.675
ISO SCORE	-	**0.400**	**0.533**	**1.800**

The macroscopical evaluation of the samples revealed no signs of hemorrage, infection or inflammation. All samples revealed, microscopically, minimal fibrosis extent, and non-detectable or rare necrosis or giant cells presence. Neoscularization was detected for all groups, as well as polymorphonucleated (PMN) cells, the latter decreasing in the latest timepoint. Following the pre-established criteria, all groups were considered biocompatible, presenting a score value contained in the "minimal or no reaction" category.

3. Discussion

FTIR analysis was performed before and after the use of different gamma irradiation conditions to evaluate any alterations in functional groups during sterilization. Comparing the spectrum of PCL scaffolds without sterilization with the spectra of sterilized PCL scaffolds, it can be seen that after gamma irradiation there were no evident modifications in the bands. These results corroborate with Tapia-Guerrero et al. and Paula et al. works that reported no significant changes in the PCL functional groups after sterilization using gamma irradiation [30]. SEM analysis was employed to determine the morphological features of the scaffolds. The microporosity observed on the surface of the filaments was caused by the material preparation method, more precisely due to the solvent addition (Biscaia). Thus, gamma irradiation had no influence on the filament morphology of PCL scaffolds.

A thorough cytocompatibility analysis was performed, including a qualitative SEM analysis of the *in vitro* seeded PCL-based scaffolds with hDPSCs. This assay allowed visualization of cellular adhesion, as well as a cellular layer formation in the 3D scaffolds, with a uniform distribution (Figure 4), thus confirming the analyzed scaffolds present potential cellular matrix conditions for 3D culture. Furthermore, SEM images of the subcutaneously implanted 3D PCL-based scaffolds in the rat animal model allowed visualization of the 3D structure integrity of the scaffolds (Figure 5), as well as tissue integration, which was validated by the histological scanning of the samples, with H&E staining (Figure 6).

As for the quantitative analysis, a Presto Blue™ viability assay confirmed the scaffolds cytocompatibility, thus sustaining the qualitative assessment by SEM analysis. All groups presented overall promising outcomes, with the 35 and 45 kGy presenting slightly better results, compared to the 25 kGy group. The control group was only considered to assess on the cellular population health, proliferation and normal behavior in culture, and direct comparisons between this group should be taken carefully, as in contrast with the tested groups, this control group is a 2D culture condition, as no matrix supporting biomaterial is considered. When considering tissue regeneration, 3D culture conditions are more reliable in mimicking the *in vivo* environmental conditions, when compared to 2D cultures. The latter are often associated with higher proliferation rates, but also with loss of diverse phenotype and metabolism alterations, thus compromising comparability with *in vivo* conditions [31, 32]. For this matter, 3D culture conditions are more likely to mimic the *in vivo* settings, as cell-extracellular, and cell-to-cell interactions are more precisely evaluated. Further, cells have variable access to nutrients and oxygen, as in *in vivo* conditions.

Considering the biocompatibility assay, the rat animal model was employed, and the scaffolds were implanted subcutaneously on the animal dorsum, considering 7- and 15-days recovery period. A semi-quantitative evaluation was performed, according to ISO 10993-6: 2016 guidelines for "Biological evaluation of medical devices, Part 6: Tests for local effects after implantation". A scoring system was applied (according to Annex E) when evaluating the biological response, as the fibrosis extent, changes in tissue morphology, necrosis presence, vascularization, fatty infiltration, and the presence of inflammatory cells. Upon euthanasia, *ex vivo* tissue presented no abnormalities, with no visible hemorrhage or inflammation/infection. A global histological score was calculated for each group and a score was determined for each experimental sample, by subtracting

 doi:10.20944/preprints202210.0202.v1

the sham group effect, associated with the intrinsic healing capacity (Table 2 and Figure 7). Microscopically, minimal fibrosis and neovascularization were detected in all samples at 7 days post implantation. Necrosis events and giant cells were rarely signalized, and mononuclear inflammatory cells (lymphocytes and macrophages) existed at a greater extent, when compared to polymorphonuclear cells, also for all groups and timepoints. A slight increase in neovascularization and decrease in fibrosis was detected at 15 days post implantation. According to the ISO 10993-6 scoring system, all samples were classified as "minimal to no reaction" at both timepoints, thus confirming its' biocompatibility ability and suitability for *in vivo* implantation. In assiction, several organs were further analyses, as to access to systemic effects through a necropsy exam and microscopic examination. Different organs were considered, as lungs, liver, heart, spleen, and pancreas. No alterations were detected.

4. Materials and Methods

4.1. Material Preparation and Devices Production & Characterization

Solid pellets of PCL (ø ~3 mm, MW 50 000, from Perstop Caprolactones (Cheshire, UK)) were dissolved in N,N Dimethylformamide (DMF, from Merck KGaA®, Germany) by solvent casting technique, using the amount of 1 g of PCL in 4 ml of DMF [25]. After the full dissolution of the PCL, the solution was deposited into petri dishes and left to dry in fume hood until solvent evaporation, for further use in a 3D printing system. The Biomate equipment was used to prepare the scaffolds [25, 33]. The 3D cylindrical scaffolds of 10 mm diameter and 2.5 height were produced using the following design parameters: 0°/90° laying pattern, 0.35 mm pore size and 0.3 mm filament diameter. Regarding processing parameters, the material was heated to 80 °C and deposited using a screw rotation velocity of 15 rpm at a working speed of 300 mm/min.

The 3D polycaprolactone (PCL) scaffolds were sterilized by gamma radiation (25 kGy, 35 kGy and 45 kGy), in a Red Perspex Dosimeters. Fourier Transform Infrared Spectroscopy (FTIR) were performed in the sterilized PCL scaffolds using Alpha FT-IR spectrometer (Bruker, Kontich, Belgium) and Opus Software. Samples were analyzed at room temperature, in a spectral range of 400-4000 cm-1, with a resolution of 4 cm-1 in a total of 64 scans.

PCL scaffolds morphology was also observed using a scanning electron microscope (SEM) (VEGA 3, TESCAN, Kohoutovice, Czech Republic) that was operated at a voltage of 15 Kv. Before observation, the scaffolds were coated with gold-palladium.

4.2. Sample Sterilization

The 3D PCL scaffolds were sterilized by gamma radiation (25 kGy, 35 kGy and 45 kGy), in a Red Perspex Dosimeters. After sterilization, the surface morphology of all 3D constructs was analyzed by using a scanning electron microscope (SEM) (VEGA 3, TESCAN) that operated at a voltage of 15 kV, after coating the powders with gold-palladium.

4.3. In vitro assays

4.3.1. Cell culture and maintenance

Human Dental Pulp stem/stromal cells (hDPSCs) obtained from AllCells, LLC (Cat. DP0037F, Lot Nº DPSC090411-01) were maintained in MEM α, GlutaMAX™ Supplement, no nucleosides (Gibco, 32561029), supplemented with 10% (v/v) fetal bovine serum (FBS) (Gibco, A3160802), 100 IU/ml penicillin, 0,1 mg/ml streptomycin (Gibco, 15140122), 2,05 µm/ml amphotericin B (Gibco, 15290026) and 10 mM HEPES buffer solution (Gibco, 15630122). All cells are maintained at 37°C, 80% humidified atmosphere and 5% CO_2 environment. Campos et al previously described the characterization of these cellular population [29].

 doi:10.20944/preprints202210.0202.v1

4.3.2. Cytocompatibility evaluation

The cytocompatibility between the cellular system and the scaffolds was assessed by a Presto Blue™ assay, to determine the impact of the sterilization intensity on the adhesion and cellular viability. The Presto Blue™ assay, a viability assessment, analyses the permeability of cells to a resazurin-based solution. This solution allows to quantify cellular viability, by modifying the media color after metabolization of the reagent by viable cells.

This assay was conducted as described in previous works [25-27]. Briefly, scaffolds are pre-hydrated in complete FBS medium for 24 hours and then seeded through dynamic seeding, where the cellular suspension is incubated with the scaffolds in a roller bank, each with a $2{,}5x10^5$ cellular suspension, for 8 hours, at 37°C, 80% humidified atmosphere and 5% CO_2 environment. Later, seeded scaffolds are transferred to a non-adherent 24 well plate and concealed with complete medium. Culture media is removed, and fresh media is added to every cultured well, at each time-point (24, 72, 120 and 168 hours). 10% (v/v) 10x Presto Blue™ cell viability reagent (Invitrogen, A13262) is added to each well and plates are incubated for 1 hour. Following, 100µl of media is transferred to a 96 well plate absorbance is read at 570 and 595nm. Dulbecco's phosphate-buffered saline solution (DPBS, Gibco, 14190169) is used to wash and remove the reagent from the wells, prior to adding fresh media. Absorbances were read at 570 nm and 595 nm with a Multiskan™ FC Microplate Photometer (Thermo Scientific™, 51119000), following manufacturing instructions. For this assay, blank wells were considered, containing the respective scaffold, but no cells. Absorbance data were collected for each well by subtracting values obtained at 595 nm from values obtained at 570 nm. Data was further corrected, by subtracting the average of the blank wells (average of 570 nm – 595 nm), from the absorbance values (570 nm – 595 nm) of each experimental well (seeded scaffolds).

A control of the cellular population was considered, where cells were seeded in 10% FBS supplemented media, directly in a tissue-treated 24 well plate, with a density of 7000 cells per cm^2, as to control cell normal growth and proliferation.

4.3.3. Scanning Electronic Microscopy (SEM)

Further, seeded scaffolds were fixated for SEM analysis, as described in previous works [25, 27]. Scaffolds were rinsed 3 times with a 0,1M HEPES (Merck®, PHG0001) buffer solution and left overnight in a fixative solution containing 2% glutaraldehyde (Merck®, G5882). A dehydration crescent alcohol series (50%, 70%, 95% and 99%) was conducted previously to the incorporation of hexamethyldisilazane (HMDS, Alfa Aesar, A15139). Samples were left overnight, as to evaporate remaining residues of the reagents.

Following, samples were coated with Au/Pd by sputtering (SPI Module Sputter Coater) for SEM analysis with a high resolution (Schottky) Environmental Scanning Electron Microscope with x-ray microanalysis and Electron Backscattered Diffraction analysis: Quanta 400 FEG ESEM / EDAX Genesis X4M in high vacuum mode.

4.4. In vivo biocompatibility assessment

Animal testing assays were conducted in conformity with the Directive 2010/63/EU of the European Parliament and the Portuguese DL 113/2013 with previous approval by the ICBAS-UP Animal Welfare Organism of the Ethics Committee (ORBEA) and by the Veterinary Authorities of Portugal (DGAV). Humane endpoints in agreement with the OECD Guidelines (2000) were followed. The *in vivo* biocompatibility assessment was performed in adult male Sasco Sprague-Dawley rats (Charles River, Barcelona, Spain) weighing 250-300g, as described in previous works [26-28]. An adequate environment for the animals was considered, with controlled temperature, humidity, and 12-12 hours light/dark cycles. Feeding included standard chow and water *ad libitum*. For the surgical procedure, anesthesia was administered intraperitoneally: Xylazine/Ketamine (Rompun®/Imalgène 1000®; 1,25mg/ 9mg per 100 g b.w.), following an aseptic skin

preparation of the dorsum. 15-20 mm long incision were performed, and scaffolds were implanted subcutaneously, following incision suture. Animals were recovered, evaluated, and returned to their housing groups. Shams were considered, where the surgical access was performed, but no medical device implanted. At 7- and 15-days recovery time, animals were subjected to anesthesia, as described above, and sacrificed, by lethal intra-cardiac injection (Eutasil® 200 mg/ml, 200 mg/kg b.w.). Skin and subcutaneous tissue was collected and fixated in 4% formaldehyde (Merck®, 100496).

Following, samples were processed for histopathological analysis, and stained with hematoxylin-Eosin (H&E). Stained sections were analyzed with a Nikon microscope (Nikon Eclipse E600) equipped with ×2, ×4, ×10 and ×40 objectives and coupled with a photo camera (Nikon Digital Sight DS-5M) equipped with a lens (Nikon PLAN UW 2X/0.06). Evaluation followed ISO-10993-6:2016 guidelines, annex E, and included inflammatory infiltration, fibrosis, angiogenesis and/or necrosis surrounding the implant. A scoring system was established, following a semi-quantitative classification of the implants as "minimal or no reaction" (score 0,0 up to 2,9), "slight reaction" (score 3,0 up to 8,9), "moderate reaction" (score 9,0 up to 15,0) or "severe reaction" (score> 15).

4.5. Statistical analysis

Statistical analysis was performed using GraphPad Prism version 6,00 for Mac OS x, GraphPad Software, La Jolla California USA. Triplicates were considered and results are presented as Mean ± Standard Error of the Mean (SE). Analysis was conducted by Two-Way ANOVA analysis with Tukey multicomparison test. Differences were considered statistically significant at $P \leq 0,05$. Results significances are presented through the symbol (*), according to the p-value, with one, two, three or four symbols, corresponding to $0.01 < p \leq 0.05$; $0.001 < p \leq 0.01$; $0.0001 < p \leq 0.001$; and $p \leq 0.0001$, respectively.

5. Conclusions

Tissue engineering of customized 3D printed medical devices relies on the premise of producing safe and implantable biomaterials, where the sterilization process plays an important role. Gamma radiation is one of the most employed sterilization processes, although the most suitable radiation level must be previously established for each study, depending on various conditions, such as the biomaterials' properties and medical condition in scope. The authors intend to investigate the potential of developing customized 3D printed PCL-based scaffolds for tracheal occlusion in CAO scenarios. For this purpose, this preliminary study was conducted, as to assess on the most suitable gamma radiation condition for PCL-based scaffolds sterilization. Higher levels from 35 to 45 kGy have presented better cytocompatibility outcomes, although 25 kGy presented equally good outcomes regarding biocompatibility after subcutaneous implantation in a rat animal model. Results suggest radiation levels of 35 kGy or 45 kGy to be safer and more suitable for the sterilization of these devices. Thus, the authors intend to continue this study, by applying these production and sterilization conditions to customized 3D-printed PCL scaffolds for trachea occlusion.

Abbreviations

AM – Additive manufacturing
CAO – Central airway obstruction
DMF – Dimethylformamide
DPBS – Dulbecco's phosphate-buffered saline solution
FBS – Fetal bovine serum
FTIR – Fourier-transform infrared spectroscopy
hDPSCs – Human dental pulp stem/stromal cells
HMDS – hexamethyldisilazane
H&E – Haematoxylin-eosin
MSCs – Mesenchymal stem cells
PCL – Polycaprolactone

SE – Standard deviation of the mean
SEM – Scanning electron microscopy

Author Contributions: Conceptualization, F.G., M.V.B., S.B., N.A., A.B. and A.C.M.; methodology, F.G., M.V.B., S.B., R.D.A., A.R., I.A., F.F., T.P., N.A., A.B. and A.C.M. software, F.G., M.V.B., S.B., R.D.A., A.C.S., and B.L.; validation, M.V.B., F.G., S.B., R.D.A., A.C.S., B.L., P.S., I.A., N.A., A.B. and A.C.M.; formal analysis, M.V.B., F.G., S.B., R.D.A., A.C.S., B.L., P.S., A.R., I.A., F.F., N.A., A.B. and A.C.M.; investigation, F.G., M.V.B., S.B., R.D.A., B.L., P.S., A.C.S., F.F., T.P., N.A. and A.C.M.; resources N.A., A.B. and A.C.M.; data curation, F.G., M.V.B., S.B., R.D.A., I.A., T.P., N.A. and A.C.M.; writing—original draft preparation, F.G., M.V.B. and S.B..; writing—review and editing, F.G., M.V.B., S.B., R.D.A, T.P., N.A., A.B. and A.C.M.; visualization, F.G., M.V.B., S.B., R.D.A. and I.A.; supervision, N.A., A.B. and A.C.M.; project administration, N.A., A.B. and A.C.M.; funding acquisition, N.A., A.B. and A.C.M. All authors have read and agreed to the published version of the manuscript. All authors had made substantial contributions to the work, with well-established division of tasks. All authors reviewed the final work and approved its submission. All authors agreed to be personally accountable for the author's own contributions and for ensuring that questions related to the accuracy or integrity of any part of the work, even ones in which the author was not personally involved, are appropriately investigated, resolved, and documented in the literature.

Funding: Mariana Vieira Branquinho (SFRH/BD/146172/2019), Ana Catarina Sousa (SFRH/BD/146689/2019), and Bruna Lopes (2021.05265.BD), acknowledge Fundação para a Ciência e Tecnologia (FCT), for financial support. Rui Damásio Alvites acknowledges the Animal Science Studies Centre (CECA), Agroenvironment, Technologies and Sciences Institute (ICETA), Porto University (UP), and FCT for the funding and availability of all technical, structural, and human resources necessary for the development of this work. The work was supported through the project UIDB/00211/2020 funded by FCT/MCTES, national funds. This research was funded by Projects PEst-OE/AGR/UI0211/2011 from FCT, and COMPETE 2020, from ANI–Projetos ID&T Empresas em Copromoção, by the project "Print-on-Organs–Engineering bioinks and processes for direct printing on organs" with the reference POCI-01-0247-FEDER-033877, by the project "Bone2Move-Development of "in vivo" experimental tech-niquesand modelling methodologies for the evaluation of 4D scaffolds for bone defect in sheepmodel: an integrative research approach" with the reference POCI-01-0145-FEDER-031146.

Institutional Review Board Statement: The study was conducted according to the guidelines of the Directive 2010/63/EU of the European Parliament and the Portuguese DL 113/2013. All the procedures were approved by the ICBAS-UP Animal Welfare Organism of the Ethics Committee (ORBEA) (Project 288/2018) and by the Veterinary Authorities of Portugal (DGAV). Humane end points were followed in agreement to the OECD Guidelines (2000).

Informed Consent Statement: Not applicable.
Data Availability Statement: The data that support the findings of this study are available from the corresponding author on request.

Acknowledgments: The authors acknowledge Daniela Silva from the Scanning Electronic Microscopy Laboratory, Materials Centre of the University of Porto.

Conflicts of Interest: The authors declare that there are no conflicts of interest regarding the publication of this article.

References

1. Fan D, Li Y, Wang X, Zhu T, Wang Q, Cai H, et al. Progressive 3D printing technology and its application in medical materials. Frontiers in Pharmacology. 2020;11:122.https://doi.org/10.3389/fphar.2020.00122
2. Graham AD, Olof SN, Burke MJ, Armstrong JP, Mikhailova EA, Nicholson JG, et al. High-resolution patterned cellular constructs by droplet-based 3D printing. Scientific reports. 2017;7(1):1-11.DOI: 10.1038/s41598-017-06358-x
3. Taylor SL, Ibeh AJ, Jakus AE, Shah RN, Dunand DC. NiTi-Nb micro-trusses fabricated via extrusion-based 3D-printing of powders and transient-liquid-phase sintering. Acta Biomaterialia. 2018;76:359-70.DOI: 10.1016/j.actbio.2018.06.015
4. Liu X, Zhao K, Gong T, Song J, Bao C, Luo E, et al. Delivery of growth factors using a smart porous nanocomposite scaffold to repair a mandibular bone defect. Biomacromolecules. 2014;15(3):1019-30.https://doi.org/10.1021/bm401911p

5. Osada H, Kojima K. Experimental tracheal reconstruction with a rotated right stem bronchus. The Annals of thoracic surgery. 2000;70(6):1886-90.DOI: 10.1016/s0003-4975(00)01847-6
6. Zani BG, Kojima K, Vacanti CA, Edelman ER. Tissue-engineered endothelial and epithelial implants differentially and synergistically regulate airway repair. Proceedings of the National Academy of Sciences. 2008;105(19):7046-51.DOI: 10.1073/pnas.0802463105
7. Daneshvar C, Falconer WE, Ahmed M, Sibly A, Hindle M, Nicholson TW, et al. Prevalence and outcome of central airway obstruction in patients with lung cancer. BMJ Open Respiratory Research. 2019;6(1):e000429.http://dx.doi.org/10.1136/bmjresp-2019-000429
8. Stratakos G, Gerovasili V, Dimitropoulos C, Giozos I, Filippidis FT, Gennimata S, et al. Survival and quality of life benefit after endoscopic management of malignant central airway obstruction. Journal of Cancer. 2016;7(7):794.DOI : 0.7150/jca.15097
9. Quach A, Giovannelli J, Chérot-Kornobis N, Ciuchete A, Clément G, Matran R, et al. Prevalence and underdiagnosis of airway obstruction among middle-aged adults in northern France: The ELISABET study 2011–2013. Respiratory medicine. 2015;109(12):1553-61.https://doi.org/10.1016/j.rmed.2015.10.012
10. Guedes F, Branquinho MV, Sousa AC, Alvites RD, Bugalho A, Maurício AC. Central airway obstruction: is it time to move forward? BMC Pulmonary Medicine. 2022;22(1):1-16.https://doi.org/10.1186/s12890-022-01862-x
11. Arami S, Jabbardarjani H, Masjedi M. Treatment of post-intubation tracheal stenosis with the Nd-YAG laser at the NRITLD. Critical Care. 2005;9(1):1-.https://doi.org/10.1186/cc3184
12. Özdemir C, Kocatürk CI, Sökücü SN, Sezen BC, Kutluk AC, Bilen S, et al. Endoscopic and surgical treatment of benign tracheal stenosis: a multidisciplinary team approach. Annals of Thoracic and Cardiovascular Surgery. 2018;24(6):oa. 18-00073.https://doi.org/10.5761/atcs.oa.18-00073
13. Saito Y, Imamura H. Airway stenting. Surgery today. 2005;35(4):265-70.https://doi.org/10.1007/s00595-004-2942-y
14. Lischke R, Pozniak J, Vondrys D, Elliott MJ. Novel biodegradable stents in the treatment of bronchial stenosis after lung transplantation. European journal of cardio-thoracic surgery. 2011;40(3):619-24.DOI: 10.1016/j.ejcts.2010.12.047
15. Freitag L, Gordes M, Zarogoulidis P, Darwiche K, Franzen D, Funke F, et al. Towards Individualized Tracheobronchial Stents: Technical, Practical and Legal Considerations. Respiration. 2017;94(5):442-56.DOI: 10.1159/000479164
16. Samat AA, Hamid ZAA, Mustapha MJ, Yahaya BH. Tissue Engineering for Tracheal Replacement: Strategies and Challenges. Springer; 2022.https://doi.org/10.1007/5584_2022_707
17. de Cassan D, Hoheisel AL, Glasmacher B, Menzel H. Impact of sterilization by electron beam, gamma radiation and X-rays on electrospun poly-(ε-caprolactone) fiber mats. Journal of Materials Science: Materials in Medicine. 2019;30(4):1-11.DOI: 10.1007/s10856-019-6245-7
18. Horakova J, Klicova M, Erben J, Klapstova A, Novotny V, Behalek L, et al. Impact of various sterilization and disinfection techniques on electrospun poly-ε-caprolactone. ACS omega. 2020;5(15):8885-92.https://doi.org/10.1021/acsomega.0c00503
19. Navarro R, Burillo G, Adem E, Marcos-Fernández A. Effect of ionizing radiation on the chemical structure and the physical properties of polycaprolactones of different molecular weight. Polymers. 2018;10(4):397.DOI: 10.3390/polym10040397
20. Augustine R, Saha A, Jayachandran V, Thomas S, Kalarikkal N. Dose-dependent effects of gamma irradiation on the materials properties and cell proliferation of electrospun polycaprolactone tissue engineering scaffolds. International Journal of Polymeric Materials and Polymeric Biomaterials. 2015;64(10):526-33.https://doi.org/10.1080/00914037.2014.977900
21. Bosworth L, Gibb A, Downes S. Gamma irradiation of electrospun poly (ε-caprolactone) fibers affects material properties but not cell response. Journal of Polymer Science Part B: Polymer Physics. 2012;50(12):870-6.https://doi.org/10.1002/polb.23072
22. Cottam E, Hukins DW, Lee K, Hewitt C, Jenkins MJ. Effect of sterilisation by gamma irradiation on the ability of polycaprolactone (PCL) to act as a scaffold material. Medical Engineering & Physics. 2009;31(2):221-6.https://doi.org/10.1016/j.medengphy.2008.07.005
23. Sadasivuni KK, Ponnamma D, Rajan M, Ahmed B, Al-Maadeed MAS. Polymer nanocomposites in biomedical engineering: Springer; 2019.ISBN: 3030047415
24. Walles T. Bioartificial tracheal grafts: can tissue engineering keep its promise? Expert Review of Medical Devices. 2004;1(2):241-50.https://doi.org/10.1586/17434440.1.2.241
25. Biscaia S, Branquinho MV, Alvites RD, Fonseca R, Sousa AC, Pedrosa SS, et al. 3D Printed Poly (e-caprolactone)/Hydroxyapatite Scaffolds for Bone Tissue Engineering: A Comparative Study on a Composite Preparation by Melt Blending or Solvent Casting Techniques and the Influence of Bioceramic Content on Scaffold Properties. International Journal of Molecular Sciences. 2022;23(4):2318.DOI: 10.3390/ ijms23042318
26. Alvites RD, Branquinho MV, Sousa AC, Amorim I, Magalhães R, João F, et al. Combined use of chitosan and olfactory mucosa mesenchymal stem/stromal cells to promote peripheral nerve regeneration in vivo. Stem cells international. 2021;2021.https://doi.org/10.1155/2021/6613029
27. Branquinho MV, Ferreira SO, Alvites RD, Magueta AF, Ivanov M, Sousa AC, et al. In Vitro and In Vivo Characterization of PLLA-316L Stainless Steel Electromechanical Devices for Bone Tissue Engineering—A Preliminary Study. International Journal of Molecular Sciences. 2021;22(14):7655.https://doi.org/10.3390/ijms22147655

28. Pinho A, Fonseca A, Caseiro A, Pedrosa S, Amorim I, Branquinho M, et al. Innovative tailor made dextran based membranes with excellent non-inflammatory response: In vivo assessment. Materials Science and Engineering: C. 2020;107:110243.https://doi.org/10.1016/j.msec.2019.110243
29. Campos J, Sousa A, Caseiro A, Pedrosa S, Pinto P, Branquinho M, et al. Dental pulp stem cells and Bonelike® for bone regeneration in ovine model. Regenerative biomaterials. 2019;6(1):49-59.https://doi.org/10.1093/rb/rby025
30. Tapia-Guerrero Y, Del Prado-Audelo M, Borbolla-Jiménez F, Giraldo Gomez D, García-Aguirre I, Colín-Castro C, et al. Effect of UV and gamma irradiation sterilization processes in the properties of different polymeric nanoparticles for biomedical applications. Materials. 2020;13(5):1090.https://doi.org/10.3390/ma13051090
31. Andersen T, Auk-Emblem P, Dornish M. 3D cell culture in alginate hydrogels. Microarrays. 2015;4(2):133-61.https://doi.org/10.3390/microarrays4020133
32. Kapałczyńska M, Kolenda T, Przybyła W, Zajączkowska M, Teresiak A, Filas V, et al. 2D and 3D cell cultures–a comparison of different types of cancer cell cultures. Archives of medical science: AMS. 2018;14(4):910.https://doi.org/10.5114/aoms.2016.63743
33. Viana T, Biscaia S, Dabrowska E, Franco MC, Carreira P, Morouço P, et al., editors. A Novel Biomanufacturing System to Produce Multi-Material Scaffolds for Tissue Engineering: Concept and Preliminary Results. Applied Mechanics and Materials; 2019: Trans Tech Publ. https://doi.org/10.4028/www.scientific.net/AMM.890.283